

Cell Reports Medicine, Volume 4

Supplemental information

Detection and targeting of splicing

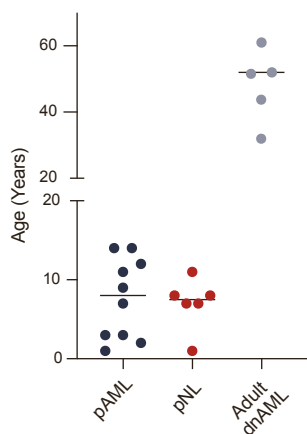
deregulation in pediatric acute

myeloid leukemia stem cells

Inge van der Werf, Phoebe K. Mondala, S. Kathleen Steel, Larisa Balajian, Luisa Ladel, Cayla N. Mason, Raymond H. Diep, Jessica Pham, Jacqueline Cloos, Gertjan J.L. Kaspers, Warren C. Chan, Adam Mark, James J. La Clair, Peggy Wentworth, Kathleen M. Fisch, Leslie A. Crews, Thomas C. Whisenant, Michael D. Burkart, Mary E. Donohoe, and Catriona H.M. Jamieson

Figure S1

A



B

NGS Hematologic Malignancy Panel

ABL1	CCND1	DDX41	GNAS	KLHL6	NRAS	RPL10	SUZ12
ASXL1	CD79B	DNM2	GNB1	KMT2A	PAX5	RPL5	TET2
ASXL2	CDKN2A_p16	DNMT1	HRAS	KMT2C	PDGFRA	RUNX1	TLR2
ATM	CDKN2A_p14	DNMT3A	IDH1	KMT2D	PDS5B	SETBP1	TP53
ATRX	CEBPA	DNMT3B	IDH2	KRAS	PHF6	SETD2	TSC2
BCL11B	CHEK2	EED	IKZF1	LUC7L2	PIK3CA	SF1	TYK2
BCOR	CNOT3	EP300	IKZF2	MAP2K1	PIM1	SF3A1	U2AF1
BCORL1	CREBBP	ETNK1	IKZF3	MEF2B	POT1	SF3B1	U2AF2
BIRC3	CRLF2	ETV6	IL2RG	MPL	PPM1D	SH2B3	NSD2
BRAF	CSF1R	EZH2	IL7R	MYD88	PRPF40B	SMARCA4	WT1
BRCC3	CSF3R	FANCL	IRF1	NF1	PRPF8	SMC1A	XPO1
BTK	CSNK1A1	FBXW7	JAK1	NFE2	PTEN	SMC3	ZRSR2
CALR	CTCF	FLT3	JAK2	NOTCH1	PTPN11	SRSF2	
CBL	CTNNB1	GATA1	JAK3	NOTCH2	RAD21	STAG2	
CBLB	CUX1	GATA2	KDM6A	NOTCH3	RB1	STAT3	
CBLC	CXCR4	GATA3	KIT	NPM1	RET	STAT5B	

Figure S1. Patient characteristics and whole exome (next generation) sequencing analyses.

Related to Figure 1.

(A) Graph of the age distribution of pediatric AML (pAML), pediatric non-leukemic (pNL) and adult *de novo* AML (adult dnAML) patient samples included in this study.

(B) NGS hematologic malignancy panel of genes (n=124) developed at UC San Diego.

Figure S2. Single cell proteogenomic detection of clonal heterogeneity in pediatric AML. Related to Figure 2.

Single cell proteogenomic analyses of three pediatric AML (pAML) patients show DNA mutation genotype, individual cell counts in each clone, and violin plots.

(A) Patient 266. Detection of SNP variants with cell counts (left) and violin plots of immunophenotyping expression of CD34, CD38, CD7 and ROR1 are shown (right).

(B) Patient 451. Detection of SNP variants with cell counts (left) and violin plots of immunophenotyping expression of CD34, CD38, CD7 and ROR1 are shown (right).

(C) Patient 678. Detection of SNP variants with cell counts (left) and violin plots of immunophenotyping expression of CD34, CD38, CD7, and ROR1 are shown (right).

Figure S3

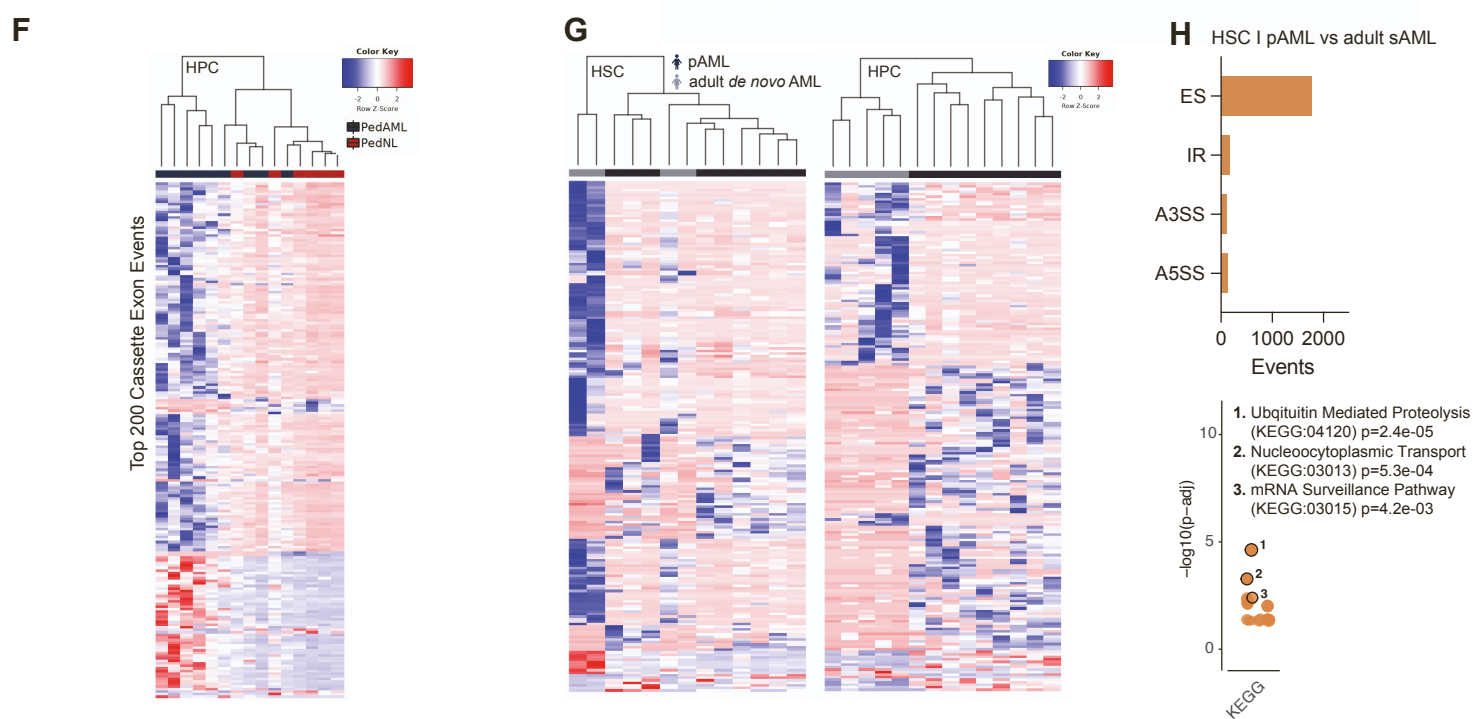
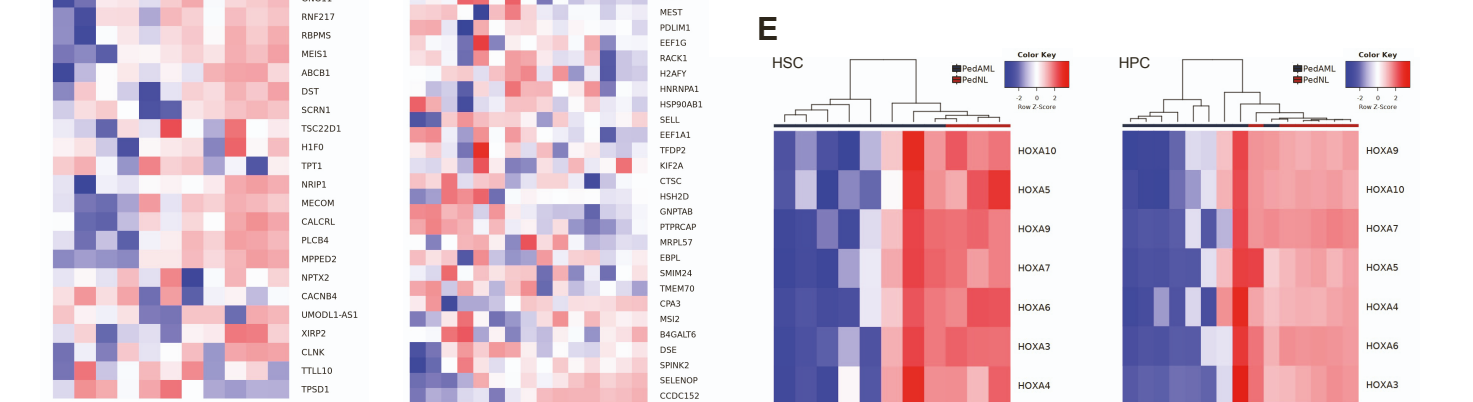
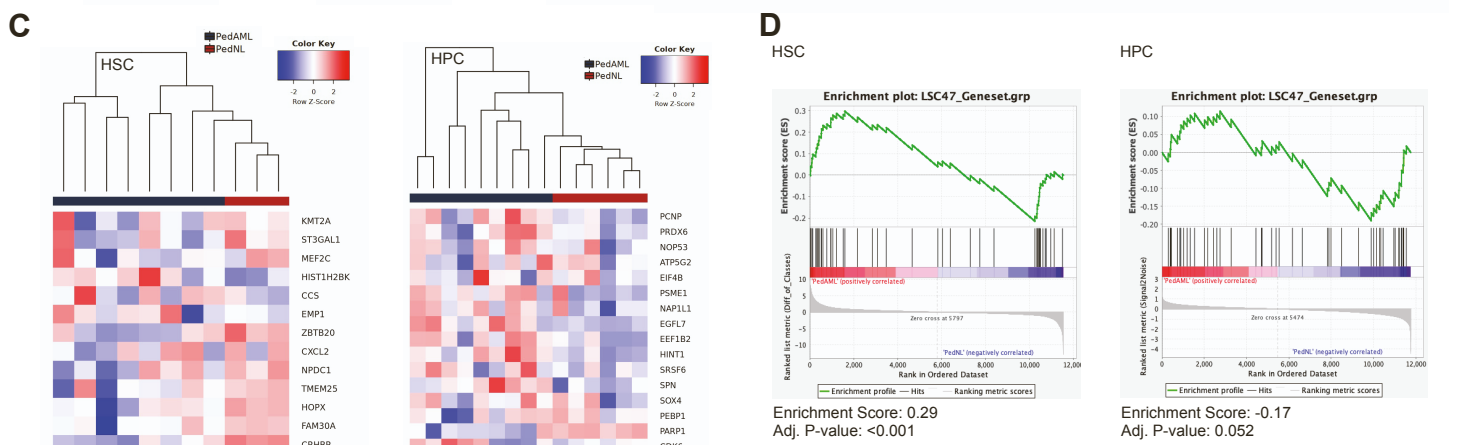
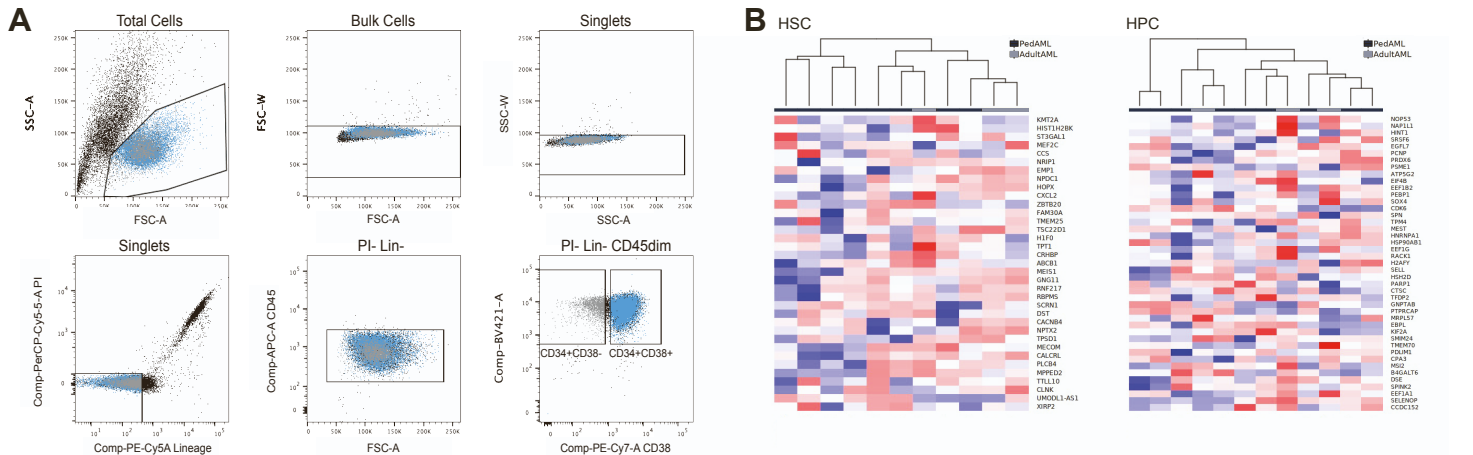
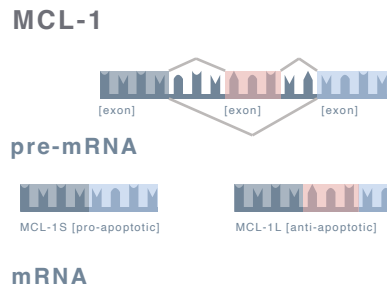


Figure S3. RNA-sequencing based hematopoietic stem cell and hematopoietic progenitor cell gene expression patterns in pediatric AML. Related to Figure 3.

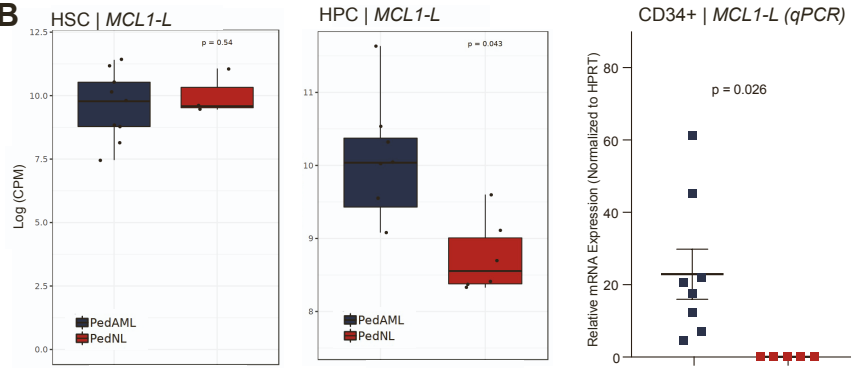
- (A) FACS gating strategy of hematopoietic stem cells (HSCs) and hematopoietic progenitor cells (HPCs).
- (B) RNA sequencing (RNA-seq) derived heatmap of normalized gene expression levels after unsupervised hierarchical clustering of pediatric AML (pAML) versus adult *de novo* AML (dnAML) HSCs (left) and HPCs (right). Genes were selected for the heatmap based on a single-cell RNA-seq study of adult dnAML.²⁹
- (C) Heatmap of normalized expression levels after unsupervised hierarchical clustering of pAML versus pediatric non-leukemic (pNL) HSCs (left) and HPCs (right).²⁹
- (D) GSEA enrichment plot of the LSC47 gene signature shows significant enrichment in pAML versus age-matched non-leukemic derived HSCs (left) and HPCs (right).
- (E) Expression of HOXA genes in pAML versus age-matched non-leukemic HSCs (left) and HPCs (right). Note, LSC47 signature is based on a study in adults.
- (F) Heatmap of top 200 distinct splice isoforms in HPCs derived from pAML versus age-matched non-leukemic cells.
- (G) Heatmap of top 200 distinct splice isoforms in HSCs (left) and HPCs (right) derived from pAML adult dnAML.
- (H) Amount of differential splicing events in HSCs derived from pAML versus adult secondary AML (sAML; top). Functional enrichment analysis of HSCs derived from pediatric AML versus HSCs derived from adult sAML (bottom). Hematopoietic stem cells (HSCs); Hematopoietic progenitor cells (HPCs).

Figure S4

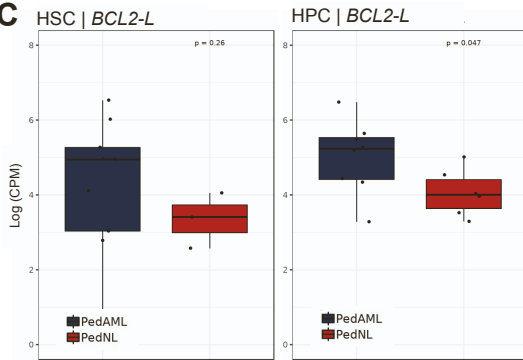
A



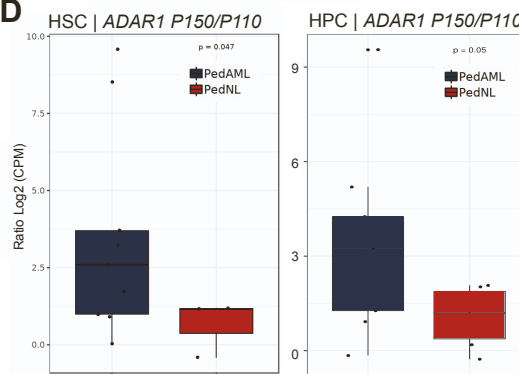
B



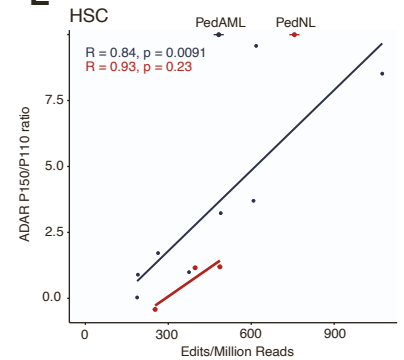
C



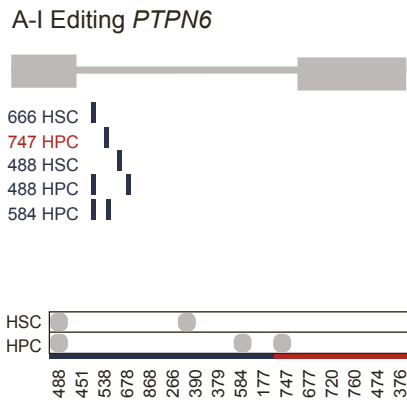
D



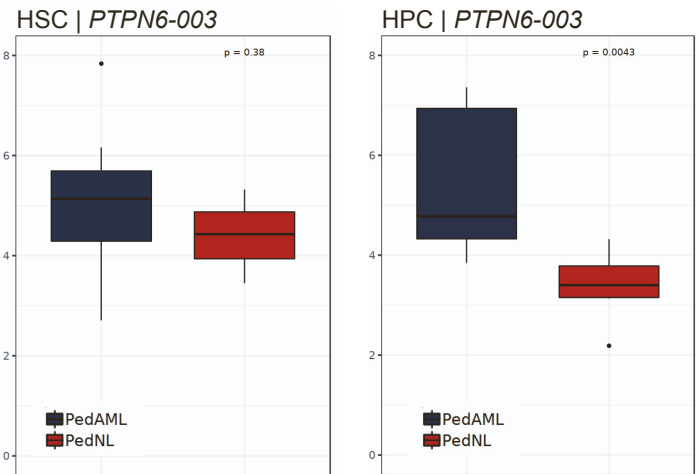
E



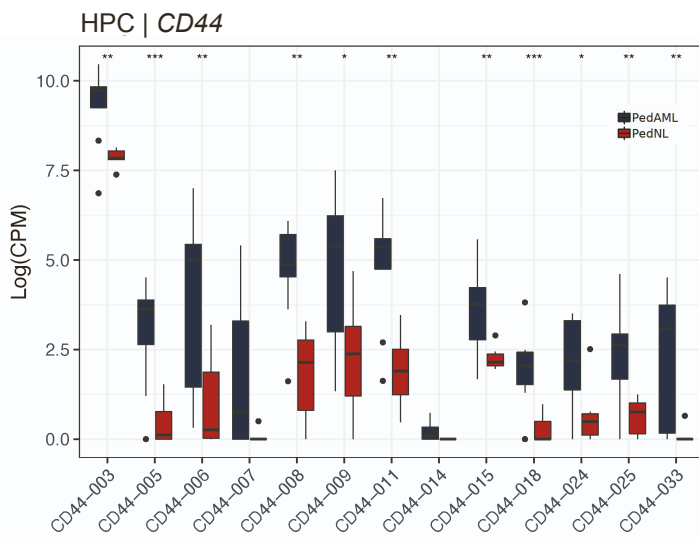
F



G



H



I

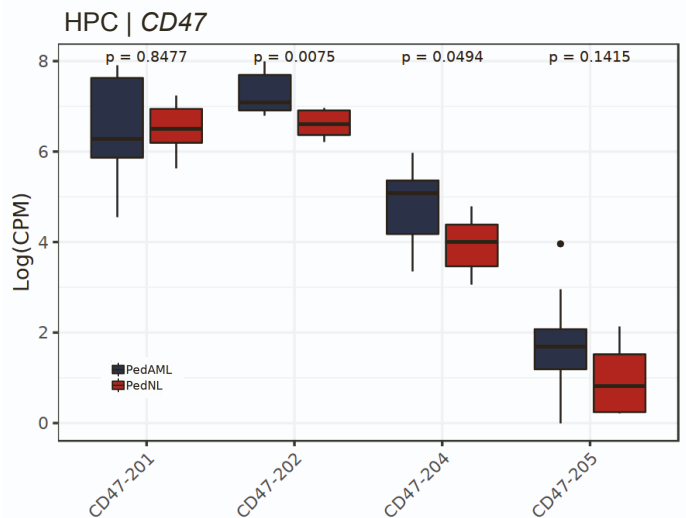


Figure S4. Differential splicing in pediatric AML hematopoietic stem cells and hematopoietic progenitor cells.

Related to Figure 4.

(A) Schematic of MCL-1 splicing.

(B) Transcript levels of *MCL1-L* based on RNA-seq of hematopoietic stem cells (HSCs) and hematopoietic progenitor cells (HPCs) in pediatric AML (pAML, n=8 biological replicates) and age-matched controls (pNL, n=5 biological replicates), and qRT-PCR of CD34⁺ selected cells derived from pAML and cord blood.

(C) RNA-seq-based expression levels of *BCL2-L* in HSCs and HPCs derived from pAML and pNL.

(D) RNA-seq-based expression levels the ratio *ADAR1 p150* to *ADAR1 p110* in HSCs and HPCs derived from pAML and pNL.

(E) Correlation of the ADAR ratio versus the number of edits per million in pAML and pNL HSCs.

(F) Adenosine to inosine (A-I) RNA editing events detected in *PTPN6*.

(G) RNA-seq-based expression levels of *PTPN6-003* in pAML and pNL HSCs and HPCs.

(H) RNA-seq-based expression of splice isoforms of *CD44* in HPCs (* - p < 0.05; ** - p < 0.01; *** - p < 0.005).

(I) RNA-seq-based quantification of splice isoforms of *CD47* in HPCs.

Figure S5

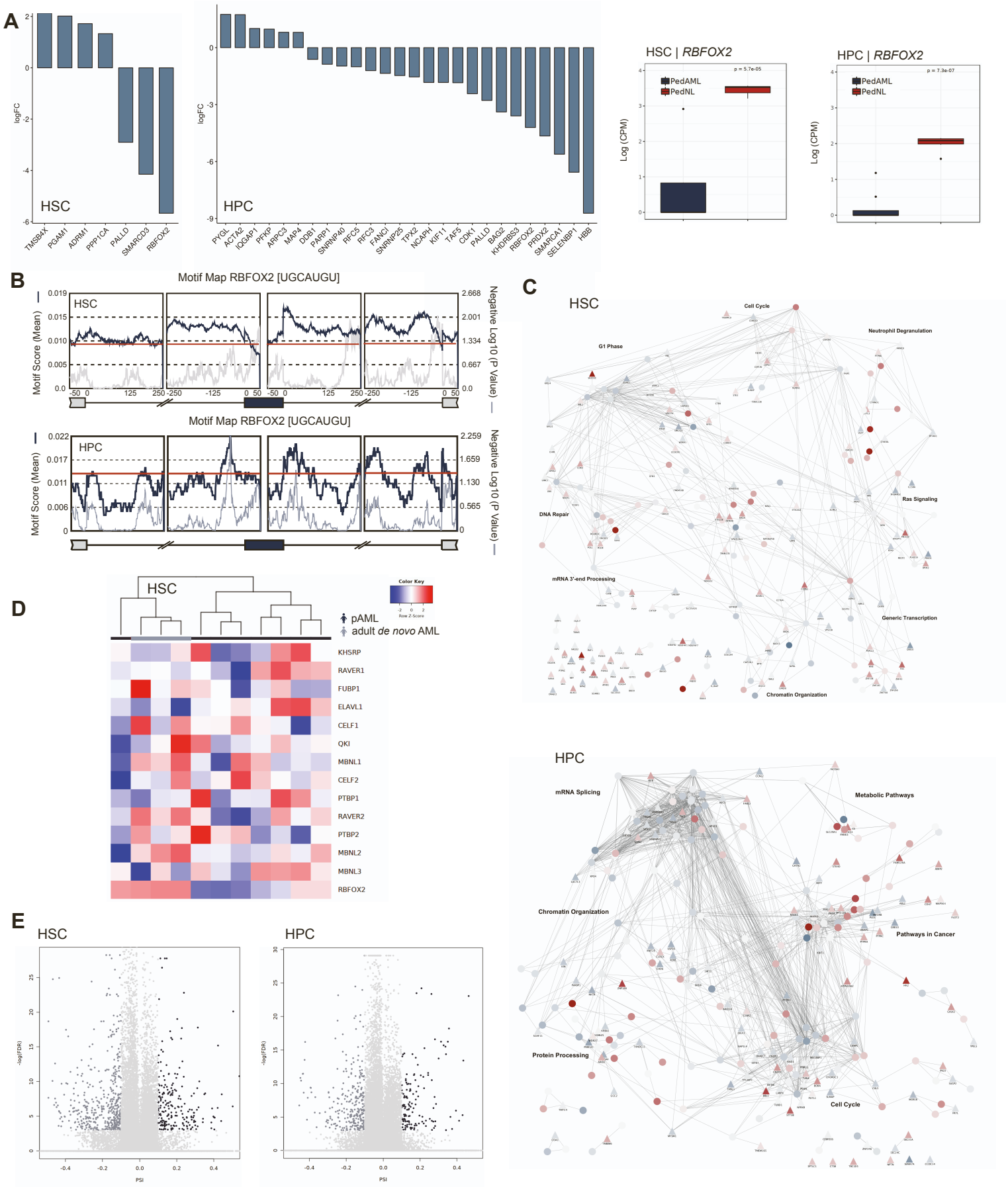


Figure S5. Decreased expression of RBFOX2 in pediatric AML and LSC survival gene expression.

Related to Figure 5.

(A) RNA-seq based quantification of significant differentially expressed human-specific spliceosome components in hematopoietic stem cells (HSCs) and hematopoietic progenitor cells (HPCs) between pediatric AML (pAML) and pediatric non-leukemic (pNL). Genes with FDR <0.05 are shown (left). RNA-seq quantification of *RBFOX2* transcript levels in HSCs and HPCs. P-values are based on student's t-test (right).

(B) rMAPS motif enrichment analysis output for RBFOX2 consensus binding site for all identified splice isoforms in HSCs (top) and HPCs (bottom; false discovery rate; FDR <0.05, percent spliced in; PSI >0.1). The blue line indicates motif score while the red line indicates Log₁₀ (p-value), and the grey line represents the background. The RBFOX2 motif score is significantly enriched if Log₁₀ (p-value) is 1.3, reminiscent of a p-value lower than 0.05.

(C) Network analysis of differentially spliced RBFOX2 target genes in pAML compared to pNL HSCs (left) and HPCs (right). Top 200 exon skipping events in this comparison were used as seeds for network propagation on the STRING high confidence interactome. Differential expression log fold change is mapped to node color. Triangles depict seed list genes and circles present associated genes.

(D) Heatmap of expression levels after unsupervised clustering of RBFOX2 associated splicing factors in pediatric AML versus adult de novo AML derived HSCs.

(E) Volcano plot highlighting RBFOX2 target genes that present differential exon usage in pediatric AML (FDR<0.05, PSI>0,1). A negative PSI reflects exon inclusion in pediatric AML while a positive PSI reflects exon skipping in pediatric AML versus adult AML-derived HSCs (left) and HPCs (right).

Figure S6

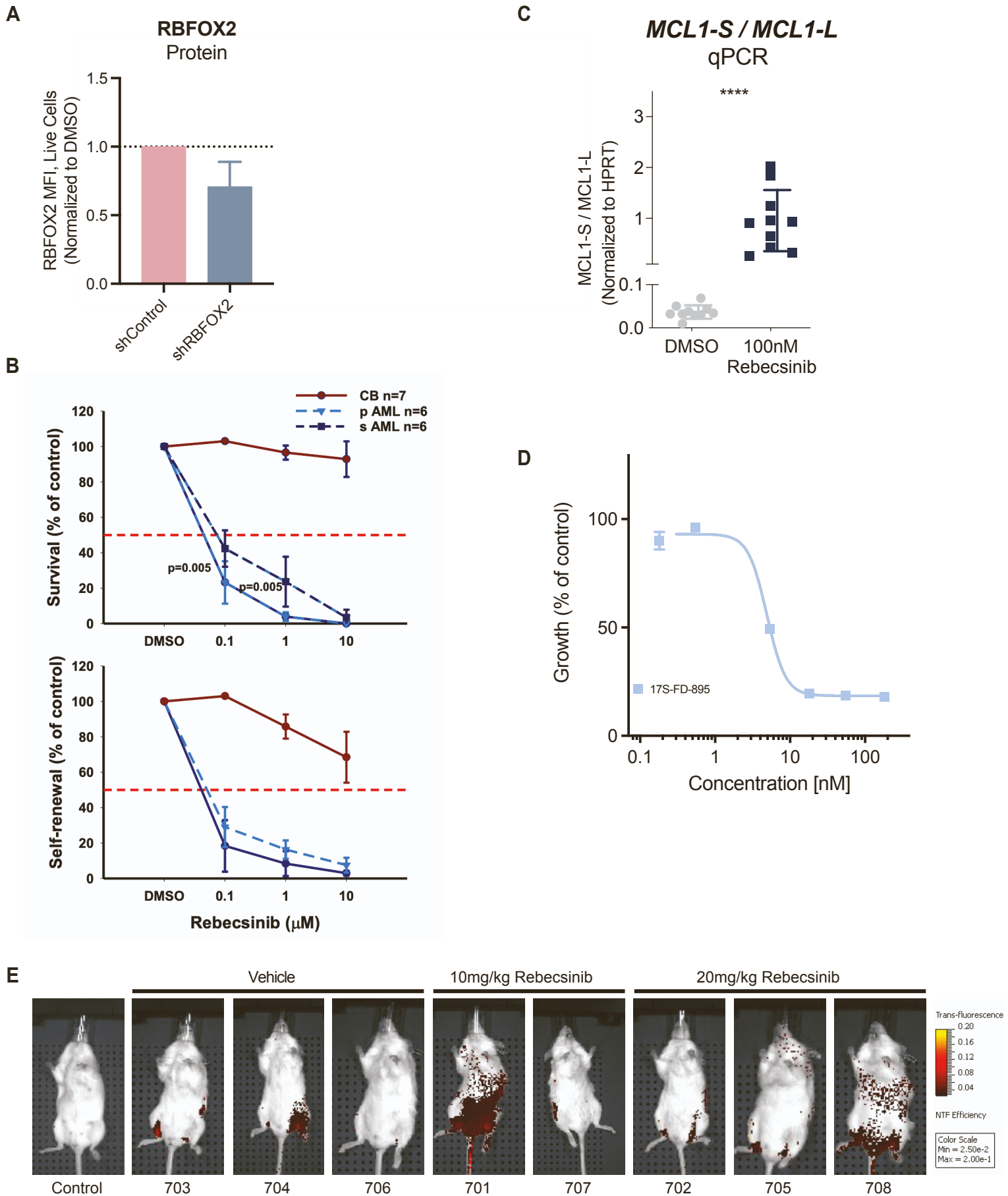


Figure S6. Rebecsinib-mediated inhibition of pediatric AML *in vitro* and *in vivo*. Related to Figure 6.

(A) Flow cytometric analysis of RBFOX2 protein levels following lentiviral shControl or lentiviral shRBFOX2 transduction of cord blood derived CD34⁺ selected cells for 48h (n=7 biological replicates).

(B) Survival and self-renewal of CD34⁺ cells derived from pediatric AML (pAML, n=6 biological replicates), cord blood or adult secondary AML (sAML, n=9 biological replicates) in long-term stromal co-cultures. These data represent the mean +/- SD for each treatment condition. Statistical analysis was performed by one-way ANOVA.

(C) qRT-PCR mRNA expression of the ratio *MCL1-S* to *MCL1-L* in pAML samples treated with 100 nM Rebecsinib; p values are based on the Mann-Whitney U test (n=10 biological replicates).

(D) MTT assay of MOLM13 cells incubated with a range of Rebecsinib (n=3 technical replicates).

(E) Live animal epifluor imaging 24h after Rebecsinib treatment.

Table S1. Patient Demographics. Related to Figure 1.

Sample ID	Gender	Age	Cell Source	Blast %	Diagnosis	Cytogenetics
488	M	7	PB	100	AML	Missing
451	M	9	PB	91	AML	Missing
538	F	14	PB	54	AML	inv(16)
678	M	1	PB	21	AML	inv(16)
868	M	2	PB	90	AML	t(15;17)
266	F	11	BM	65	AML	CEBPA
390	M	12	BM	54	AML	t(8;21)
379	F	3	PB	91	AML	Missing
584	M	14	PB	52	AML	Missing
177	M	3	BM	30	AML	t(8;21)
1474	M	52	PB	83	de novo AML	inv(16), KIT, NRAS
251	F	32	BM	32	de novo AML	inv(16), NRAS, KRAS
023	M	52	BM	56	de novo AML	CEBPA, NRAS, WT1
220	M	44	BM	37	de novo AML	MLL-PTD, STAG2
682	M	61	BM	34	de novo AML	t(8;21)
747	F	7	BM	NA	Complete Remission	NA
677	F	7	BM	NA	Healthy Donor	NA
720	F	8	BM	NA	Healthy Donor	NA
760	M	1	BM	NA	Lymphoma without BM involvement	NA
474	M	11	BM	NA	Lymphoma without BM involvement	NA
376	M	8	BM	NA	Lymphoma without BM involvement	NA

Male (M); Female (F); Age in years; Bone marrow (BM); Peripheral blood (PB); Acute myeloid leukemia (AML)

Table S4. Primer Sequences. Related to Figure 6.

Transcript	Species	Primer FW sequence (5'-3')	Primer REV sequence (5'-3')
HPRT	Human	TCAGGGATTTGAATCATGTTTGTG	CGATGTCAATAGGACTCCAGATG
MCL1-L	Human	AGACCTTACGACGGGTTGG	AATCCTGCCCCAGTTTGTTA
MCL1-S	Human	GAGGAGGACGAGTTGTACCG	ACTCCACAAACCCATCCTTG